Supplementary information

Supplementary Table 1. Model names and host institutions of the CMIP5 models used in this study.

Model	Institute
ACCESS1.0	Commonwealth Scientific and Industrial Research Organisation and Bureau of Meteorology, Australia
BCC_CSM1.1	Beijing Climate Center, China Meteorological Administration, China
BCC_CSM1.1m	Beijing Climate Center, China Meteorological Administration, China
CCSM4	National Center for Atmospheric Research, USA
CESM1-CAM5	National Center for Atmospheric Research, USA
CMCC-CM	Centro Euro-Mediterraneo per I Cambiamenti Climatici, Italy
CNRM-CM5	Centre National de Recherches Meteorologiques/Centre Europeen de Recherche et Formation Avancees en Calcul Scientifique, France
CSIRO-Mk3.6	Commonwealth Scientific and Industrial Research Organisation, Australia
FGOALS-g2	LASG, Institute of Atmospheric Physics, Chinese Academy of Sciences; and CESS, Tsinghua University, China
FGOALS-s2	LASG, Institute of Atmospheric Physics, Chinese Academy of Sciences, China
GFDL-CM3	Geophysical Fluid Dynamics Laboratory, USA
GISS-E2-R	NASA Goddard Institute for Space Studies, U
HadGEM2-A	Met Office Hadley Centre, UK
INM-CM4	Institute for Numerical Mathematics, Russia
IPSL-CM5A-MR	Institut Pierre-Simon Laplace, France
MIROC5	Atmosphere and Ocean Research Institute (The University of Tokyo), National Institute for Environmental Studies, and Japan Agency for Marine-Earth Science and Technology, Japan
MPI-ESM-LR	Max Planck Institute for Meteorology, Germany
MPI-ESM-MR	Max Planck Institute for Meteorology, Germany

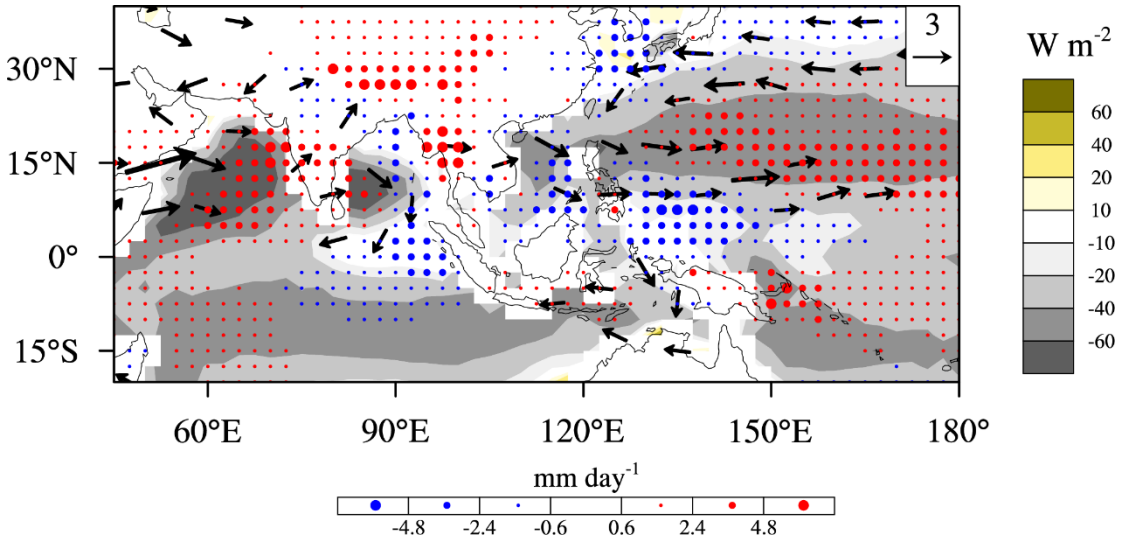

Supplementary Figure 1. Ensemble mean biases of surface energy gain (shading), precipitation (dots), and 850hPa wind (vectors; units in m s^{-1}) during JJA (1984–2005) in the atmosphere-only models. Only vectors with wind speed larger than 1.8 m s^{-1} are shown.

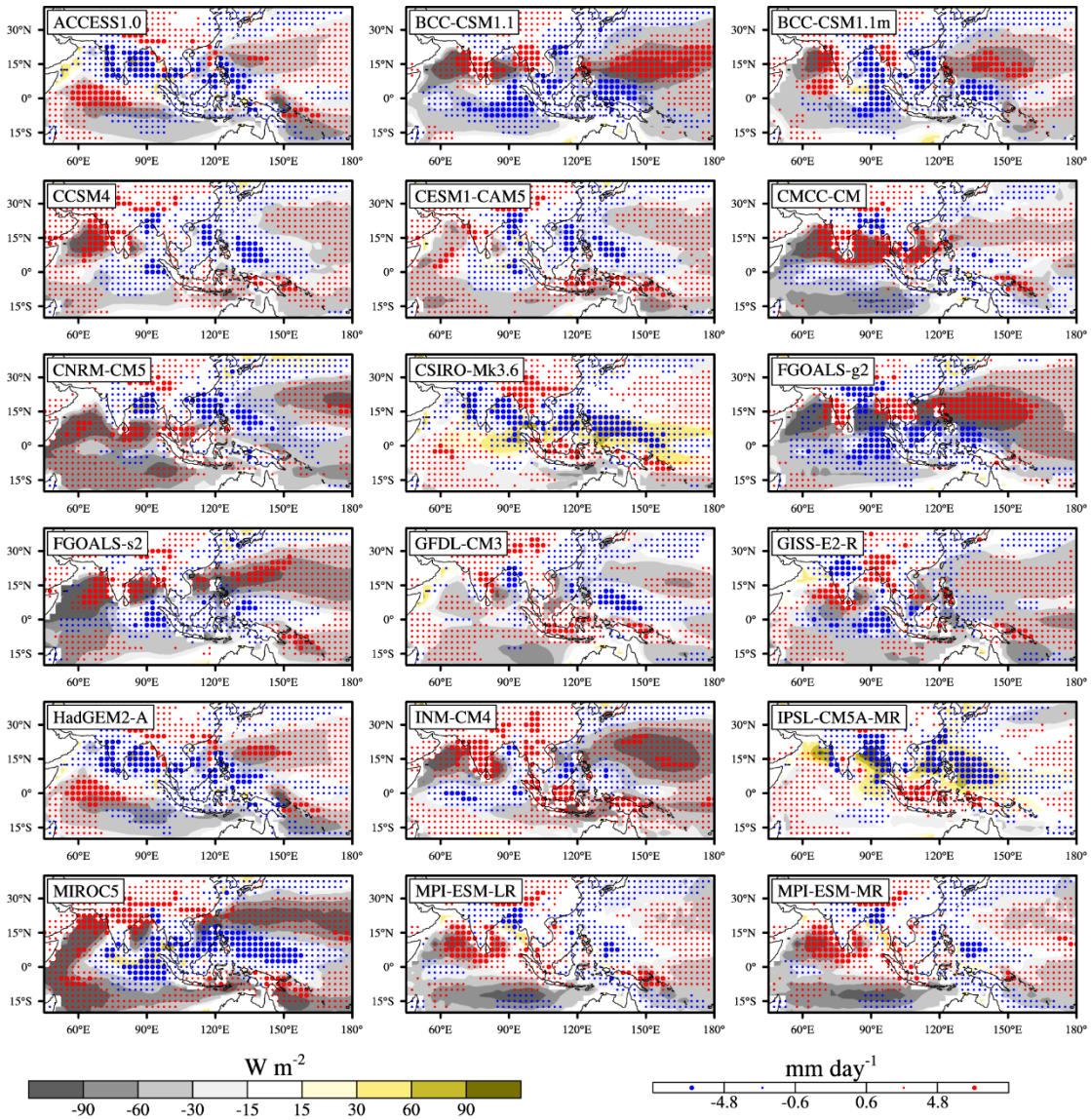

Supplementary Figure 2. Atmosphere-only model biases of surface energy flux (shading) and precipitation (dots) during JJA (1984–2005) in each individual model.

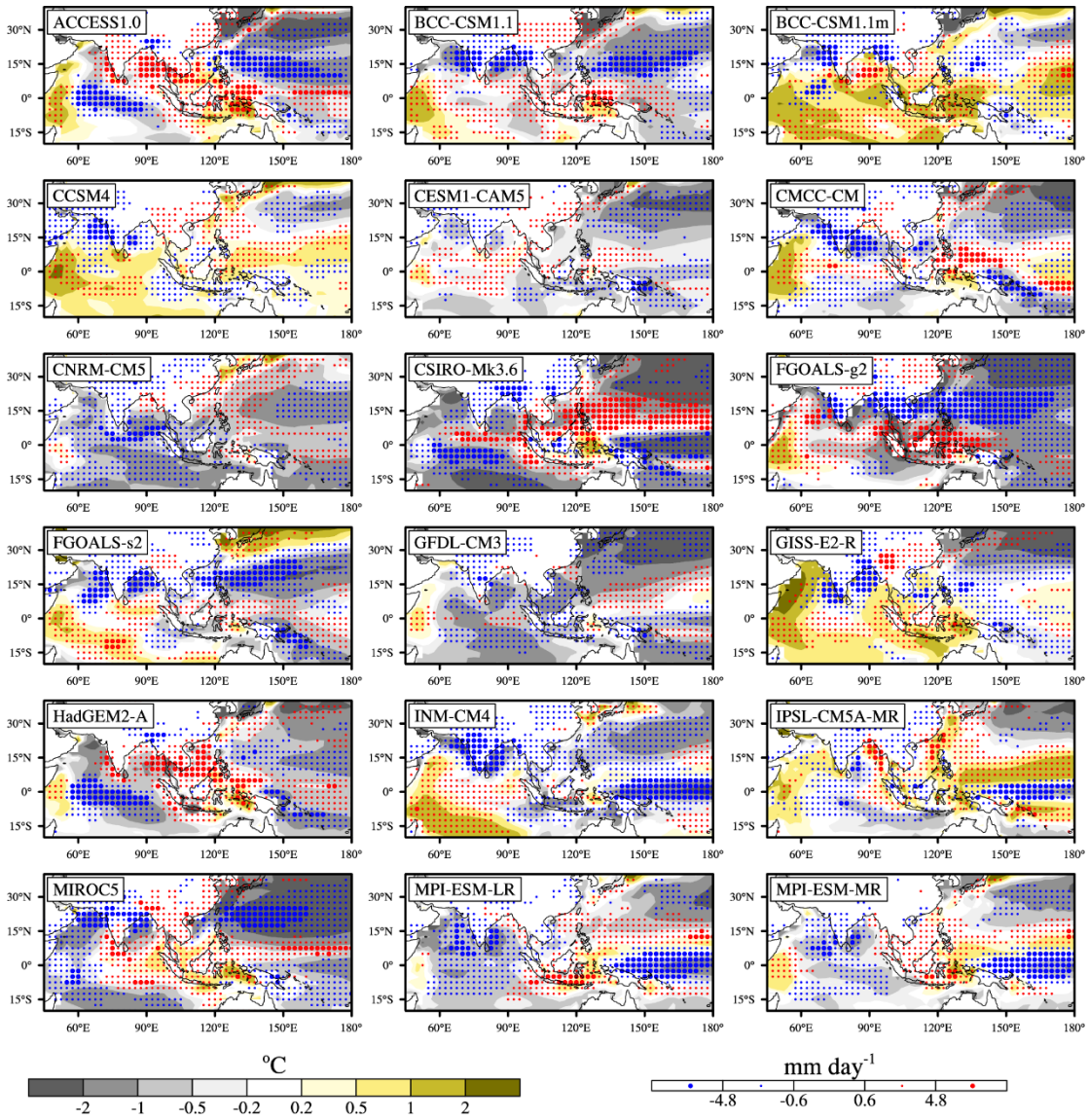

Supplementary Figure 3. Coupling-induced changes (i.e. coupled model results minus atmosphere-only model results) of SST (shading) and precipitation (dots) during JJA (1984–2005) in each individual model.

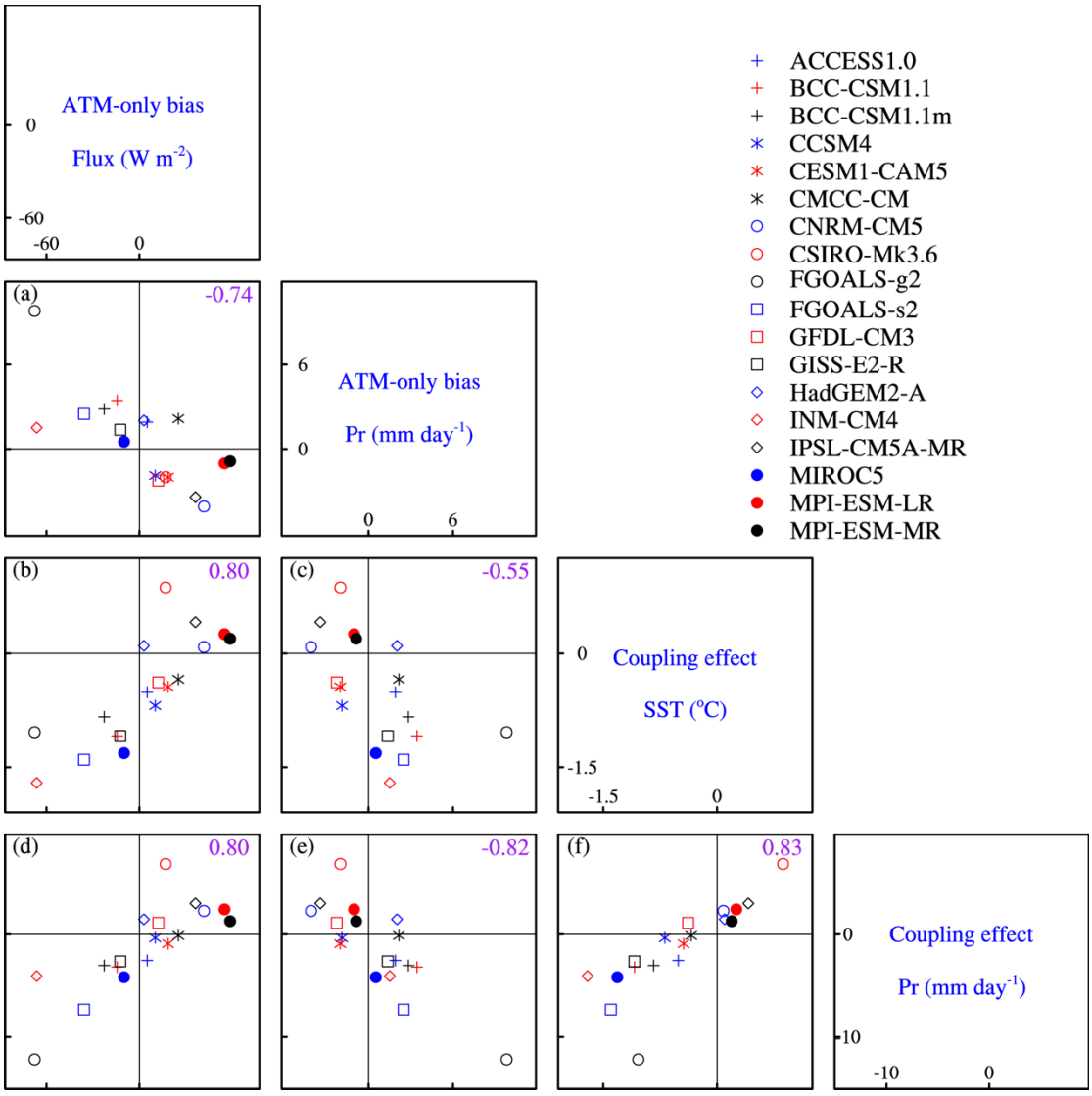

Supplementary Figure 4. Scatter plots between any two of four variables listed in the diagonal panels based on the NWP minus the southern tropical Indian Ocean averages (see Fig. 1a for the region information) from the 18 CMIP5 models. In each panel the correlation coefficient between the two variables is given at the top-right corner, with purple indicating statistical significance at the 95% confidence level.

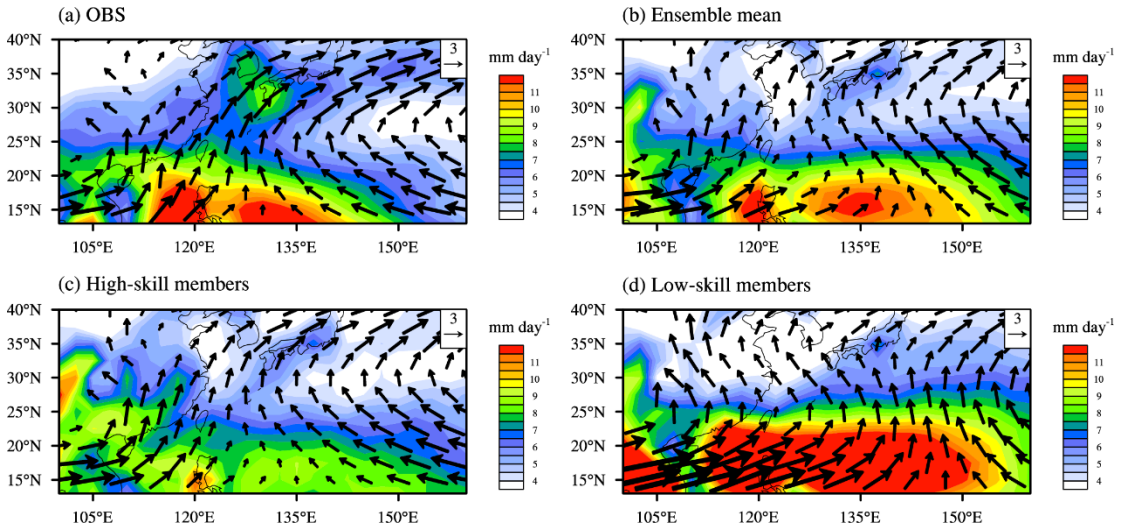

Supplementary Figure 5. Spatial distributions of climatological mean precipitation (shaded) and 850-hPa winds (vectors) during JJA (1984-2005) from (a) observation, (b) ensemble mean of all the 18 atmosphere-only models, and ensemble mean of the 3 atmosphere-only models with the (c) highest and (d) lowest skills in simulating the surface energy gain over NWP.

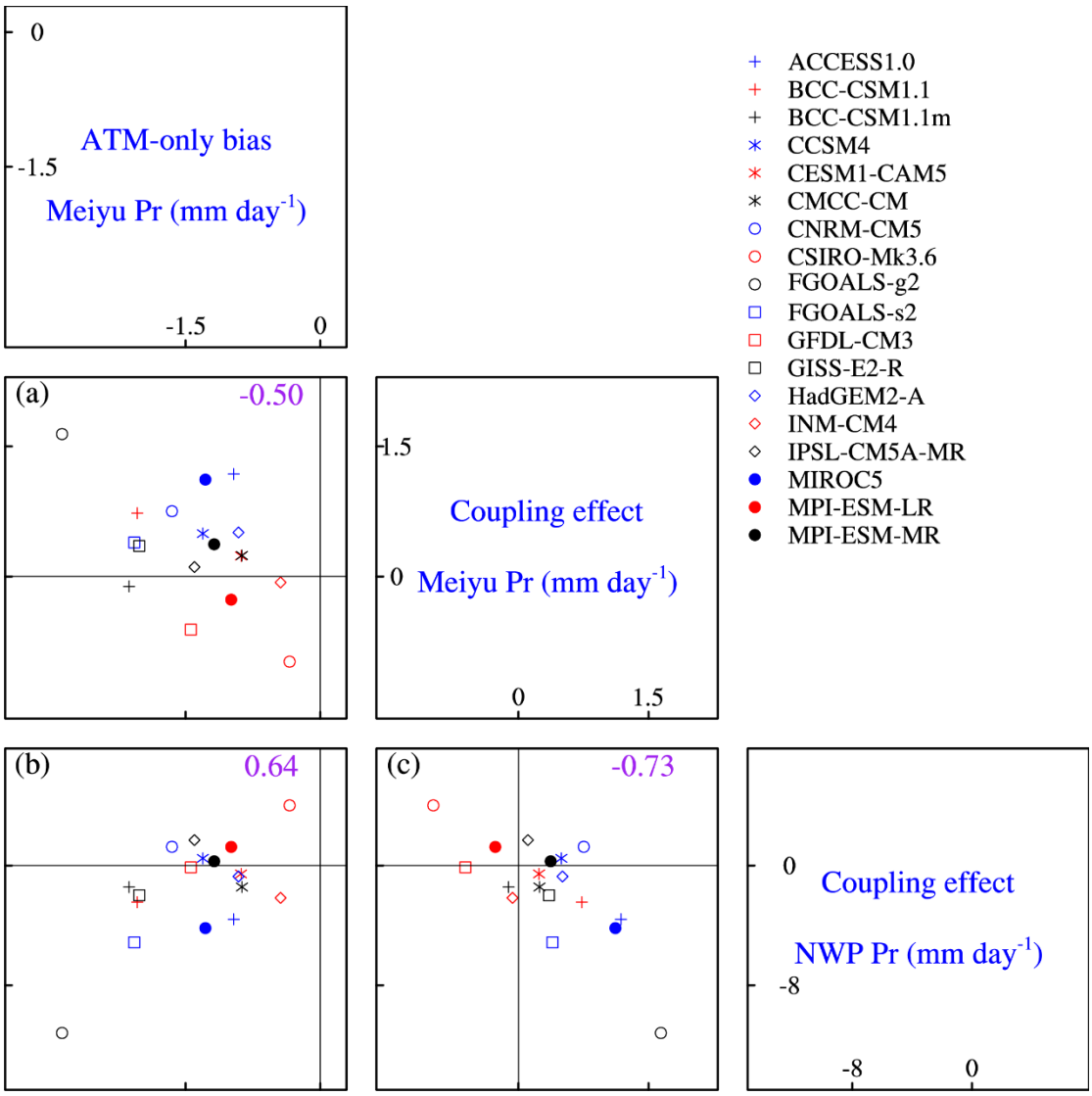

Supplementary Figure 6. Scatter plots between any two of three variables listed in the diagonal panels based on the climatological mean results from the 18 CMIP5 models. The three variables include the atmosphere-only bias of precipitation over the Meiyu front region (see Fig. 1a) and the coupling-induced precipitation changes over the Meiyu front region and over NWP (see Fig. 1a). In each panel the correlation coefficient between the two variables is given at the top-right corner, with purple indicating statistical significance at the 95% confidence level.

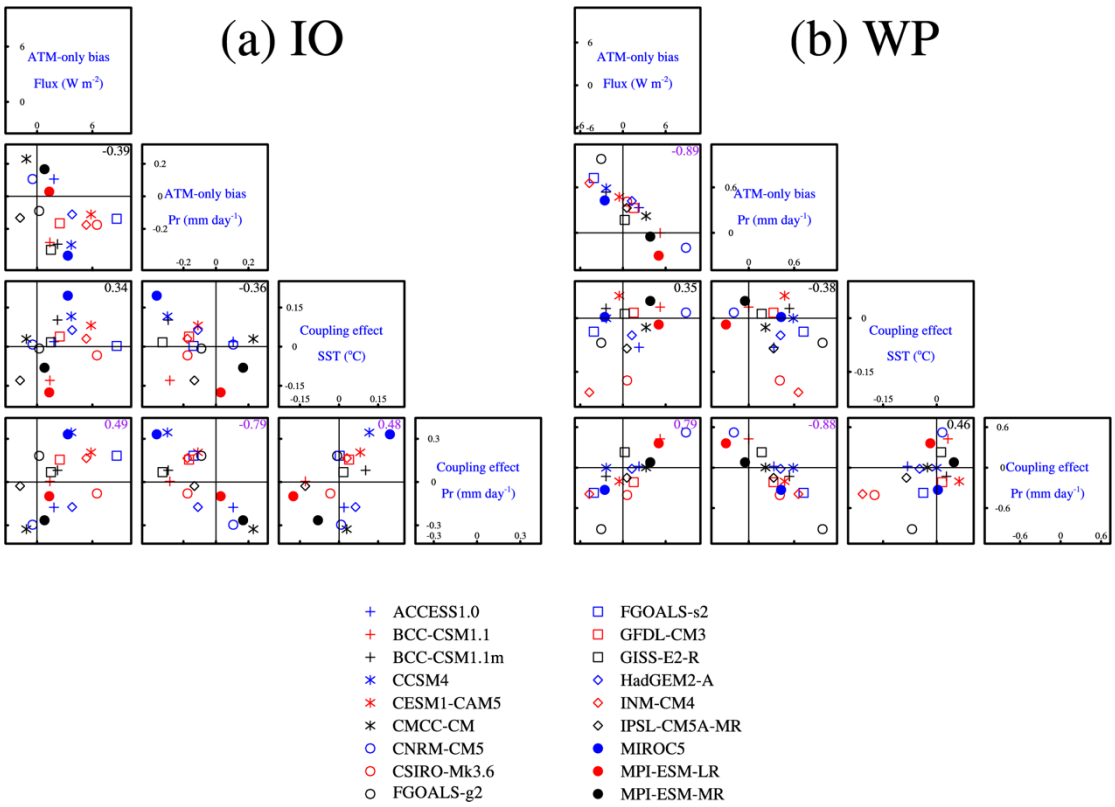

Supplementary Figure 7. Scatter plots between any two of four variables listed in the diagonal panels based on the results averaged over (a) Indian Ocean and (b) the western Pacific from the 18 CMIP5 models. The four variables and numbers in each panel have the same meaning as that in Fig. 2 except that the variables are for the regressed interannual patterns.

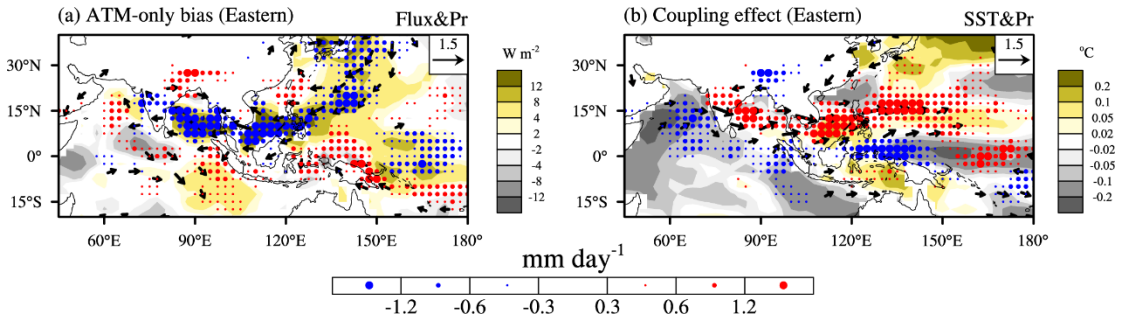

Supplementary Figure 8. (a) Atmosphere-only model biases of the regressed interannual patterns of surface energy flux (shading), precipitation (dots), and 850hPa wind (vectors; units in m s^{-1}) and (b) coupling-induced changes (coupled model minus atmosphere-only model results) of the regressed interannual patterns of SST (shading), precipitation (dots), and 850hPa wind (vectors; units in m s^{-1}) during JJA (1984–2005) in the eastern-type models. Only vectors with wind speed larger than 0.4 m s^{-1} are shown.

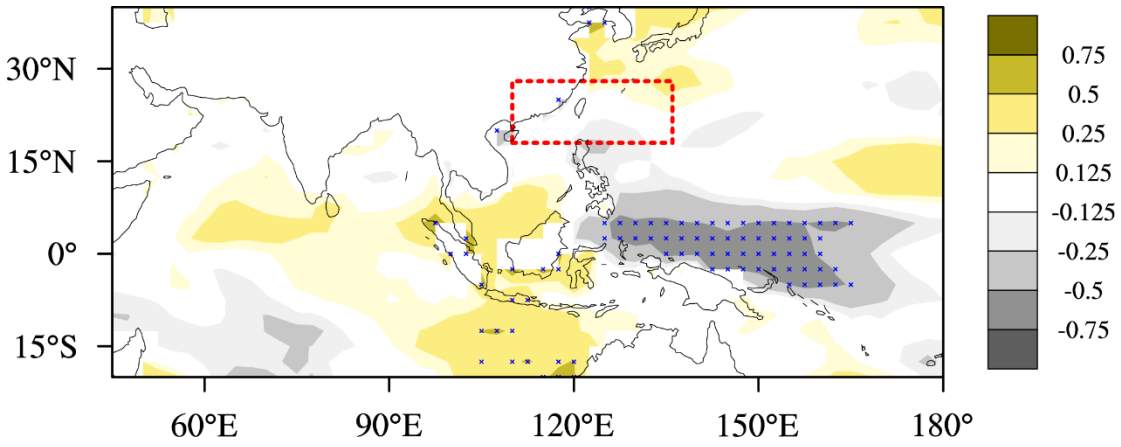

Supplementary Figure 9. Correlation coefficient between coupling-induced precipitation change averaged over southern China and adjacent oceans (red box) with coupling-induced SST change at each grid point, with blue crosses indicating statistical significance at the 95% confidence level.

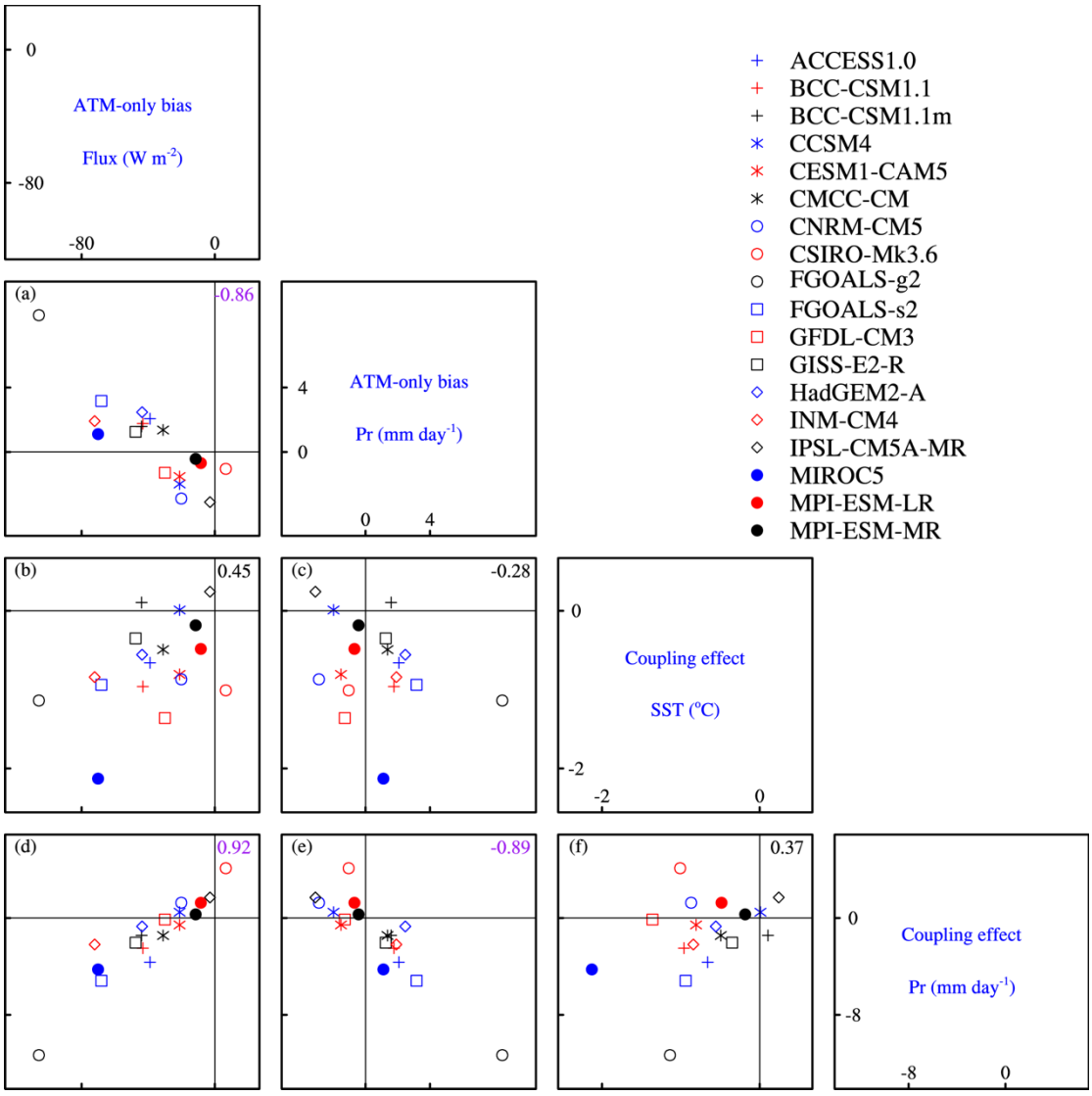

Supplementary Figure 10. Same as Fig. 2 except that the surface energy gain (i.e. the first variable) is based on the sum of shortwave radiation, longwave radiation, latent heat flux, and sensible heat flux.

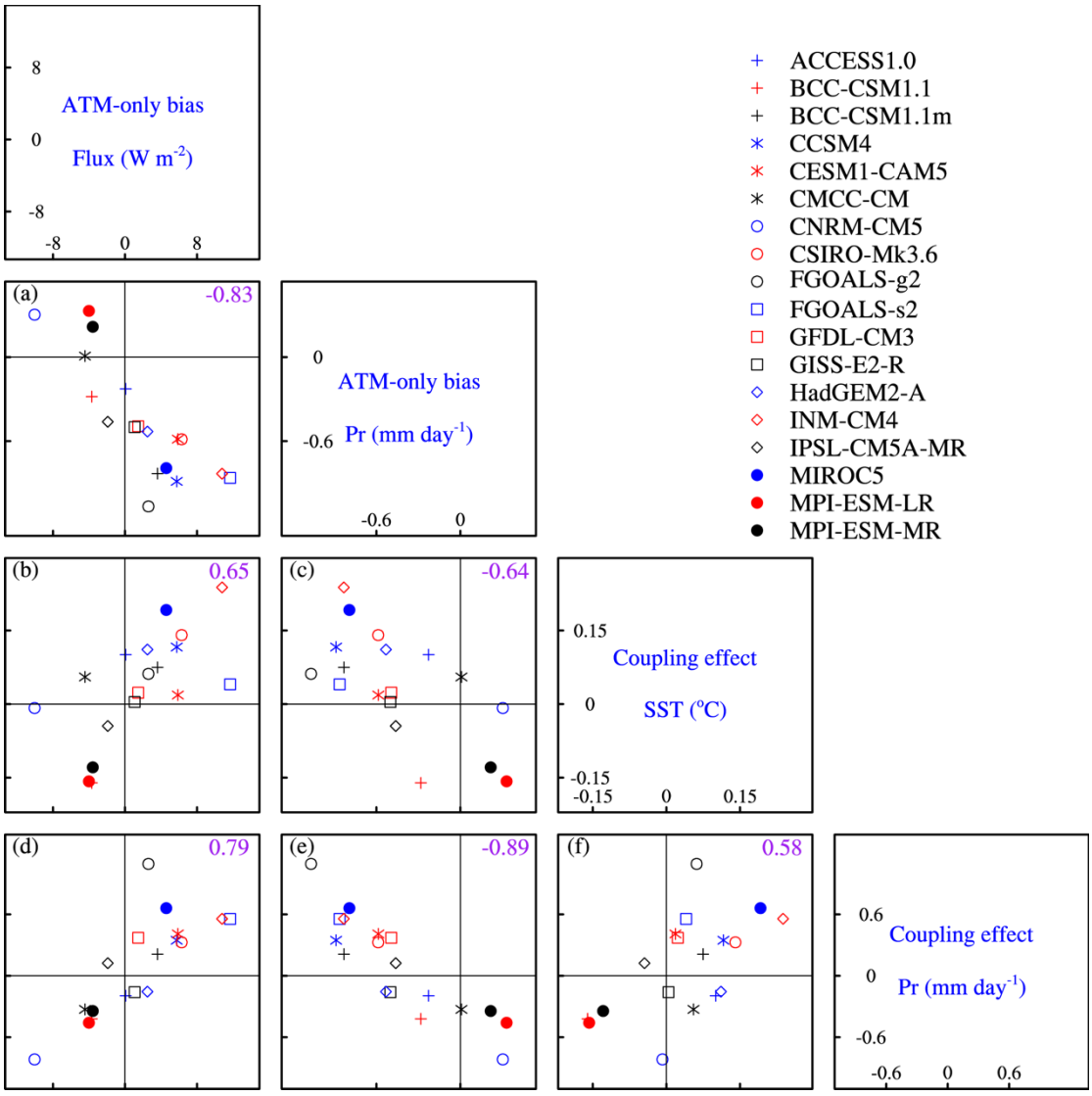

Supplementary Figure 11 Same as Fig. 4 except that the surface energy gain (i.e. the first variable) is based on the sum of shortwave radiation, longwave radiation, latent heat flux, and sensible heat flux.

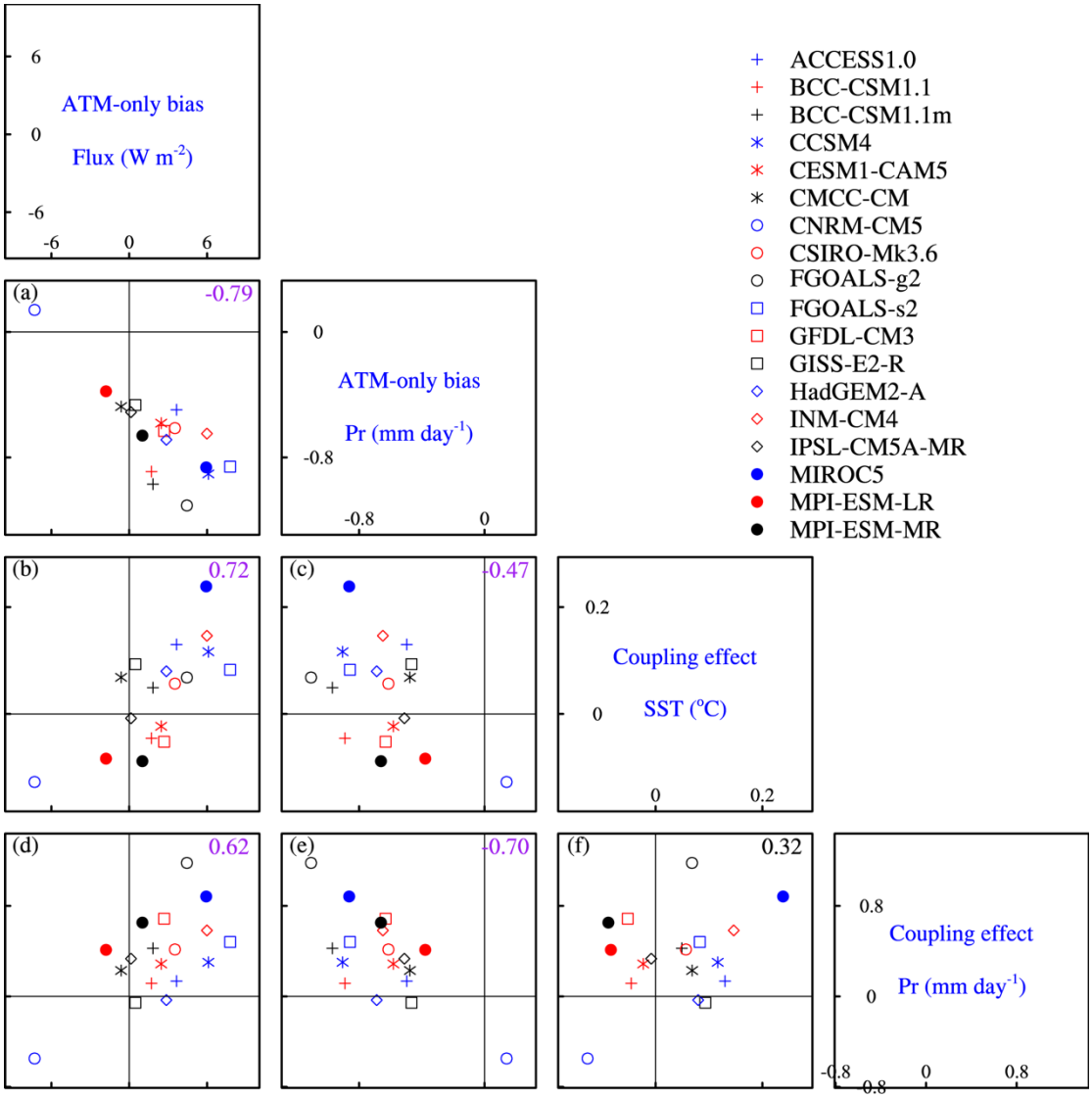

Supplementary Figure 12. Same as Fig. 4 except that the results in the atmosphere-only models are regressed against the observed standardized EASM index. Note that the western Pacific defined here is slightly smaller than that in Fig. 4 because of the different spatial features of the EOF patterns.

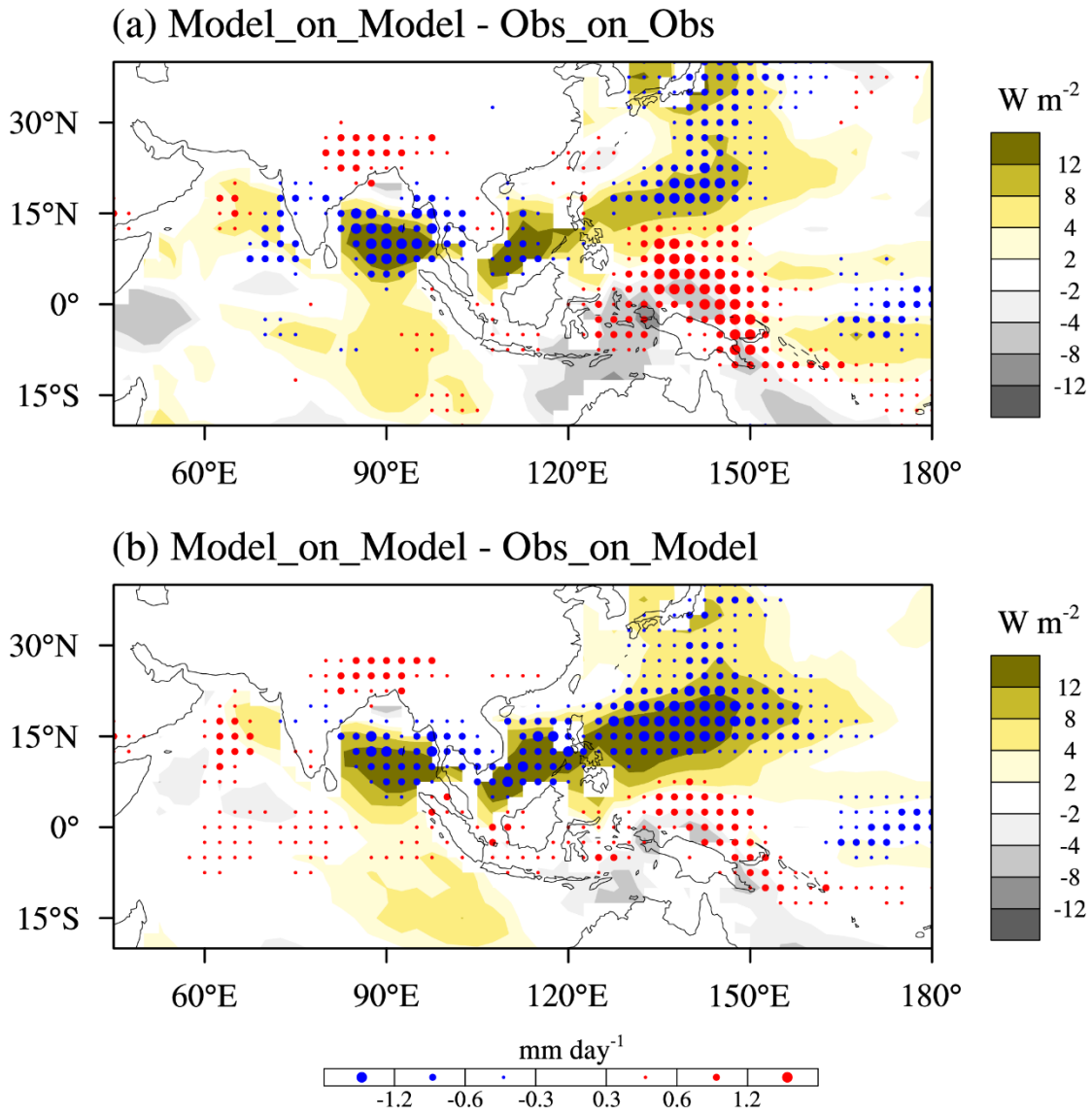

Supplementary Figure 13. (a) Ensemble mean of atmosphere-only model biases of the regressed interannual patterns for surface energy gain (shading) and precipitation (dots). (b) Same as (a) except that the results in observation are first regressed against the simulated standardized EASM index in each individual atmosphere-only model and then averaged.

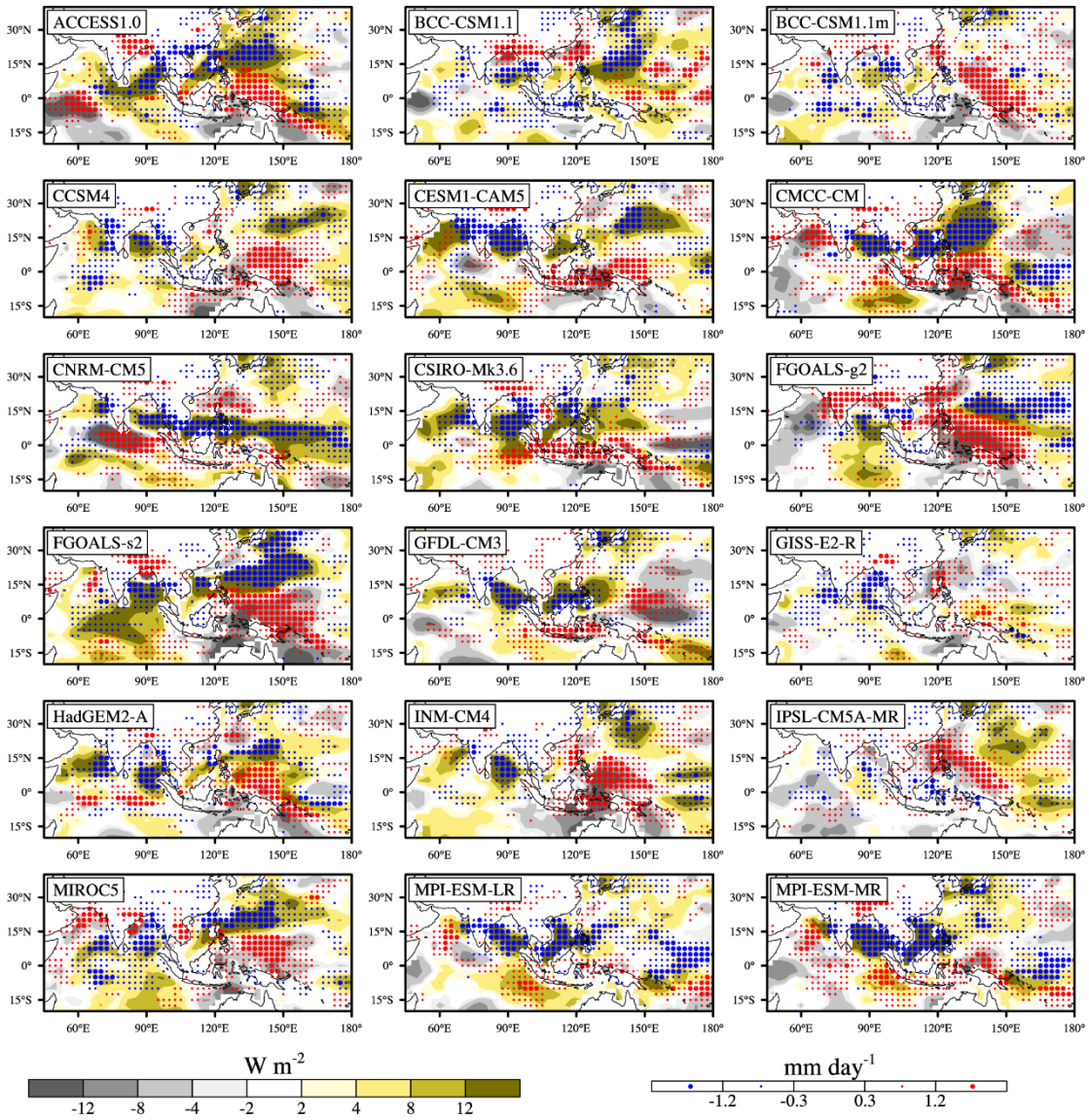

Supplementary Figure 14. Biases of the regressed interannual patterns of surface energy gain (shading) and precipitation (dots) in each individual atmosphere-only model.

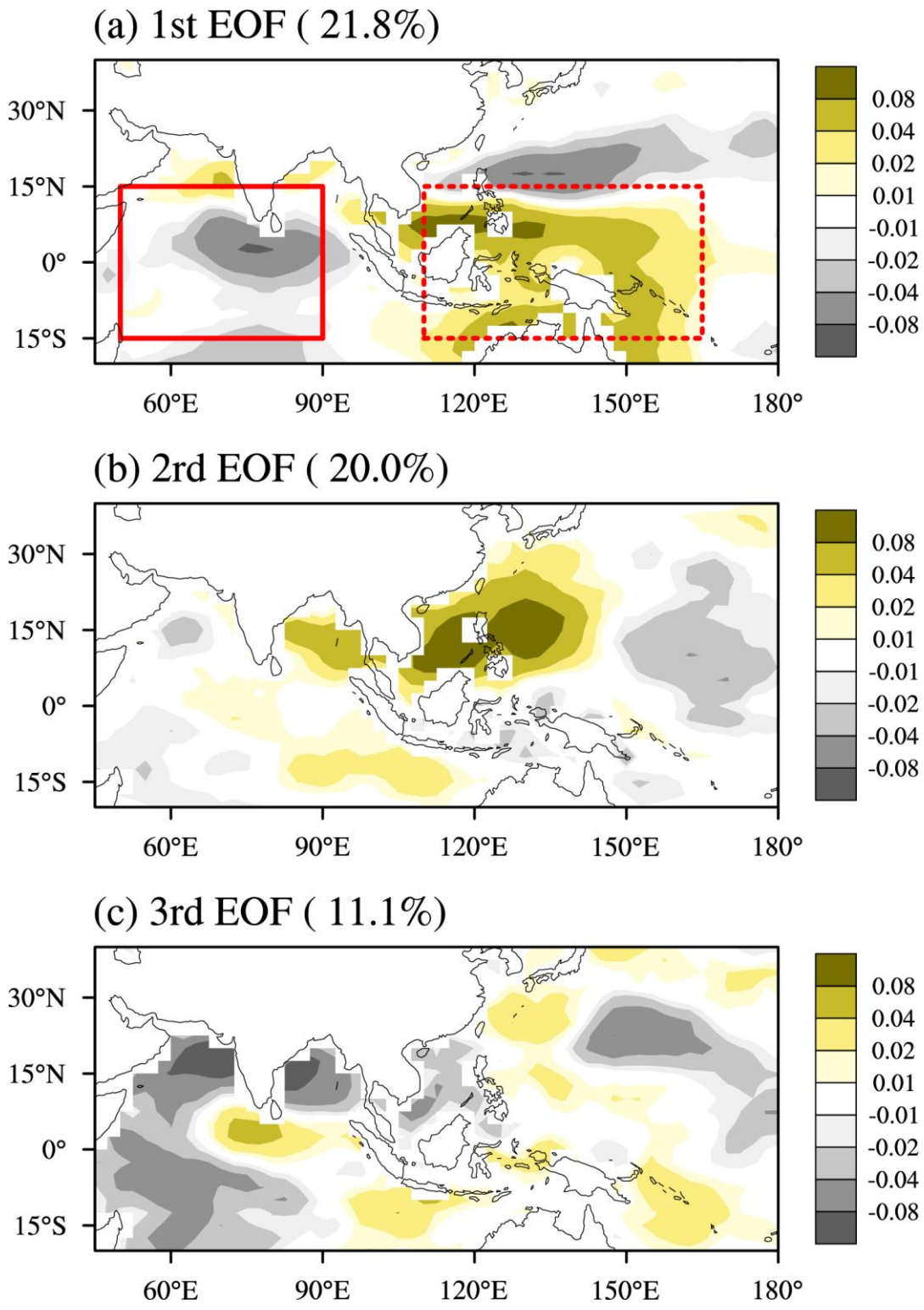

Supplementary Figure 15. The (a) first, (b) second, and (c) third EOF eigenvectors of the inter-model differences of the regressed interannual patterns for surface energy gain in the 18 atmosphere-only models.